CONF-9206325--1

PNL-SA--21022

DE93 005034

LIGHT EXTINCTION IN THE ATMOSPHERE

N. Laulainen

June 1992

Presented at the
IAU/ICSU/UNESCO Exposition
in the Adverse Environment
Impact on Astronomy
June 30 - July 2, 1992
Paris, France

MASTER

Prepared for
the U.S. Department of Energy
under Contract DE-AC06-76RLO 1830

Pacific Northwest Laboratory
Richland, Washington 99352

LIGHT EXTINCTION IN THE ATMOSPHERE

ABSTRACT

Atmospheric aerosol particles originating from natural sources, such as volcanos and sulfur-bearing gas emissions from the oceans, and from human sources, such as sulfur emissions from fossil fuel combustion and biomass burning, strongly affect visual air quality and are suspected to significantly affect radiative climate forcing of the planet. During the daytime, aerosols obscure scenic vistas, while at night they diminish our ability to observe stellar objects. Scattering of light is the main means by which aerosols attenuate and redistribute light in the atmosphere and by which aerosols can alter and reduce visibility and potentially modify the energy balance of the planet. For the astronomer, light scattering by aerosols affects "seeing" in two major ways: 1) through diminishing the intensity of the stellar object being observed, and 2) through increasing sky brightness by scattering light from unwanted sources, such as city lights and moonlight.

Trends and seasonal variability of atmospheric aerosol loading, such as column-integrated light extinction or optical depth, and how they may affect potential climate change have been difficult to quantify because there have been few observations made of important aerosol optical parameters, such as optical depth, over the globe and over time and often these are of uneven quality. Thus, to address questions related to possible climate change, there is a pressing need to acquire more high-quality aerosol optical depth data. Extensive deployment of improved solar radiometers over the next few years will provide higher-quality extinction data over a wider variety of locations worldwide. An often overlooked source of turbidity data, however, is available from astronomical observations, particularly stellar photoelectric photometry observations. With the exception of the Project ASTRA articles published almost 20 years ago, few of these data ever appear in the published literature. This paper will review the current status of atmospheric extinction observations, as highlighted by the ASTRA work and augmented by more recent solar radiometry measurements. The paper will conclude with a request for additional information on available atmospheric extinction data archived by the astronomical community and with a few recommendations for how these data can be used to augment current IGBP/Global Change research activities.

Introduction

How often have you gone out on a clear night to look at the stars only to find that just a few of the brightest ones can be seen without difficulty? Poor "seeing" is also the bane of the astronomer. Often he tries to observe stars from mountain tops away from population areas to minimize atmospheric effects that cause poor "seeing". Reduced "seeing" is the result of increased sky brightness and the attenuation of starlight by the atmosphere. Both effects decrease the contrast between the stars and the sky and limit our ability to see them.

What are the causes of these two effects? Particles suspended in the atmosphere (aerosols) are the primary culprits. Aerosols, especially in the size range found most commonly in the atmosphere (roughly between 0.1 and 1 μm), are very effective scatterers and, to a lesser extent, absorbers of visible light. These scattering and absorption processes not only reduce the intensity of starlight (extinction), but also increase sky brightness by reflecting light from other bright sources, such as the moon and cities.

Aerosols also affect climate forcing and visibility in much the same way that they affect "seeing". In fact, the same aerosol optical parameters come into play for all three phenomena--namely, the vertical column- (or horizontal path-) integrated extinction coefficient or optical depth and a parameter related to angular scattering phase function of individual particles. The "acid rain" phenomena, so much in the news during the last decade, also has its origins from these same optically active particles.

With respect to climate forcing, Charlson et al. (1992) assert that present-day levels of aerosols (mostly sulfate particles) arising from human activities can exert a direct radiative influence on climate that is comparable, but opposite in sign, to that resulting from the increase of greenhouse gases since preindustrial times. Thus, anthropogenic aerosols may have offset global greenhouse warming and may mask the detection of the onset of the greenhouse effect of CO_2 and other greenhouse gases. They further stress that differences in the geographical and seasonal distributions between aerosol and greenhouse

climate forcing, however, preclude any simple compensation. Because 90% of anthropogenic SO_2, one of the main precursor gases of atmospheric sulfate aerosol, is emitted in the Northern Hemisphere, the resultant forcing is expected to be exerted predominantly there. There are still large uncertainties, however, in estimating the magnitude and geographical distribution of aerosol radiative forcing.

Visibility impairment by anthropogenic aerosols impacts both transportation safety and aesthetic appreciation of scenic vistas. Improvement of visibility is an important national goal in the United States and understanding the current visibility situation and its sensitivity to future emission changes requires improved data on aerosol optical properties, size distribution and chemical composition. Integrated measures that influence the "visibility" of an object or scene are the path extinction and the path-integrated radiance (air brightness as a result of light scattered into the line of sight) between the observer and the object. Although human perception of visibility impairment is largely a subjective response, all indices of visual air quality ultimately reduce to the light extinction coefficient, and its response to varying relative humidity, as the single, generally accepted, objective measurable variable.

What is the origin of atmospheric aerosols and what is their chemical and physical nature? Aerosols originate either directly by mechanical injection processes (smoke and ash from fires, wind blown dust, ash from volcanic eruptions) or indirectly by gas-to-particle conversion processes (chemical reactions, condensation from the vapor phase) in the atmosphere. Generally, aerosols produced indirectly (or secondary aerosols) have a dominant effect on radiative transfer in the atmosphere because of two key properties: 1) Their diameters are in the size range 0.1 - 1 μm, which means they will remain suspended for several days to a week in the lower atmosphere until they are washed out by rain and for months to years in the stratosphere. 2) This same size range produces the most efficient scattering of visible light. In many locations, sulfate aerosol is the dominant chemical species. It is formed from the conversion of SO_2, a byproduct of fossil fuel combustion, to sulfuric acid. It is also formed from the oxidation of natural sulfur compounds emitted from the oceans. The most significant point about sulfur emissions is that the

current anthropogenic sulfur flux is roughly three times the global natural flux, which, as discussed above, contributes to the present estimates of aerosol direct radiative climate forcing (Charlson et al. 1992). In some locations, other aerosol chemical species, such as elemental carbon from combustion processes or organic compounds, could have significant impacts on climate forcing or visibility.

Trends and seasonal variability of atmospheric aerosol burdens and their effect on climate forcing have been difficult to quantify because of a lack of reliable observations over the earth and over time. Addressing the aforementioned large uncertainties in the magnitude and geographical distribution of aerosol radiative forcing requires greater global coverage and higher frequency of sampling of key radiative forcing parameters from satellite observations. Connecting the satellite-derived data set with the important radiative characteristics of the atmosphere requires the development of a complementary data set of the local and column-integrated aerosol optical, chemical, and physical properties from ground-based observing stations. Aerosol optical depth is one of the important column-integrated quantities needed for this purpose.

Solar radiometry has been the principal method for obtaining aerosol optical depth data. It should be noted that while the earlier data sets were limited to only a few locations with limited coverage over time and were of uneven quality as a result of instrumental drift and calibration uncertainties, they have provided the impetus for the development of improved radiometers, such as the new multi-spectral rotating shadowband radiometers (Harrison 1991; LeBaron et al. 1989). These newer instruments should provide much-needed improvement in the quality of the data and, because of the relatively low cost per unit and the automation of the data reduction tasks, should allow for wide geographic deployment. Some results taken with this type of instrument will be presented in this paper.

An often overlooked source of optical depth data is also available from astronomical observations, particularly from stellar photoelectric photometry. Two decades ago, a project was started at the University of Washington t examine the utility of modern photoelectric photometry as a tool for monitoring

atmospheric transparency and aerosol light extinction. This project, Astronomical and Space Techniques for Research on the Atmosphere (ASTRA) culminated in a series of three articles on the analyses of atmospheric extinction data obtained by astronomers (Laulainen et al. 1977; Laulainen 1977; Taylor et al. 1977). These articles focused on time trends, seasonal variations, and vertical distribution of light extinction.

Because modern photoelectric photometry dates back to only 1960 (or somewhat earlier), the ASTRA analyses were limited to a data series of about one decade, roughly 1960 to 1970. The trend analysis showed an increase in optical depth at 550 nm of ~0.01 ± 0.01 per decade [combined data from Kitt Peak National Observatory (KPNO) and Lick Observatory]. By making some reasonable assumptions about the vertical distribution of aerosols and extinction efficiency (extinction coefficient per unit mass concentration), this extinction trend translated into a aerosol mass loading trend (to within a factor of 2) of ~10 ± 10 $\mu g\ m^{-3}$. It should be noted that the large uncertainty in this result includes a no-change trend in mass loading over that decade. Seasonal variation in optical depth (at 550 nm) were noticeable at many sites, with amplitudes of ~0.02 at Cerro Tololo Interamerican Observatory (CTIO), KPNO, Lick Observatory and McDonald Observatory, but nearly absent at others. Site geography and altitude also played a significant role in observed mean optical depths. Most of the mean extinction data was bracketed by profiles derived from other independent observations in remote maritime background air and derived from a LOWTRAN-type model atmosphere with a surface (sea level) visual range of ~20 km.

In the two decades since the publication of the ASTRA papers cited above, numerous volcanic eruptions have perturbed the aerosol loading of the stratosphere, and anthropogenic sulfur emissions have about doubled. One might expect that the atmospheric extinction data base from various observatory sites would have also grown during this period and would be rich in information on aerosol trends and perturbations. Few of these data, with the exception of those reported by Lockwood and Thompson (1986), for example, have appeared in the published literature.

Analysis techniques have also improved since the ASTRA study, particularly those applied to the analysis of noisy data. One example is a robust statistical technique known as locally-weighted regression and smoothing scatterplots or LOWESS (Cleveland 1979). This technique was used by Pearson et al. (1988) and Michalsky et al. (1990) to extract the El Chichon stratospheric signal from optical depths determined from solar radiometric observations at Rattlesnake Mountain in Eastern Washington. Lockwood and Thompson (1986) likewise used an exploratory data analysis software package to compare ordinary and volcanically induced variations in atmospheric extinction over the period 1972-1985.

Although the available astronomical literature on atmospheric light extinction is scanty, it does appear worthwhile to repeat an ASTRA-like investigation of photoelectric stellar photometry data. A survey of this type would be of immense value in aiding the research community in assessing trends and variability in atmospheric transparency for the three-decade period, 1960-1990. It remains to be seen, however, how many data sets can be retrieved, since, as Lockwood (private communication) cautions, the CCD (charged-coupled detector) era in astronomical photometry seems to have put an end to long-term extinction series in many places.

With this rather long introduction, the remainder of this paper focuses on a review of the current status of atmospheric light extinction observations. It will focus on summarizing and comparing the results of Michalsky et al. (1990) using solar radiometry and of Lockwood and Thompson (1986) using stellar photometry, as well as presenting salient results of the ASTRA work in the context of present understanding. It will also present some tantalizing results of Jäger (1991, 1992) of stratospheric aerosol observations and trends obtained using a lidar. The paper will conclude with a request for assistance from the astronomical community to identify available atmospheric extinction data and with a few recommendations for how these data can be used to augment current IGBP/Global Change research activities.

Measurement of Atmospheric Light Extinction

All techniques for the measurement of light extinction are based on the Bouguer-Beer-Lambert law, which expresses the loss of radiant intensity of a beam traversing a scattering and absorbing medium, in this case the atmosphere, as an exponentially decreasing function of airmass m and optical depth δ. Astronomers use the magnitude system (a logarithmic scale) for measuring intensities and astronomical atmospheric extinction κ and δ differ only by about 8% (i.e., $\delta = 0.921\ \kappa$). The differences between these two measures of light extinction are usually small in comparison to magnitude of their variability and uncertainty.

Because gas molecules and particles can absorb and scatter light, these light extinction quantities may be further broken down into contributions from molecular (Rayleigh) scattering, molecular absorption (e.g., water vapor, ozone), particle scattering and particle absorption. For much of the discussion in this paper, either total optical depth δ_e or aerosol optical depth δ_{ep} will be used.

Deriving values of δ (or κ) requires the determination of the instrumental outside-the-atmosphere intensity (I_o) for each wavelength band. If the atmospheric aerosol burden is invariant in time and uniformly distributed over the observing site, multiple observations of intensity I over a range of airmass values m can be used to determine I_o and δ by means of the Langley method, which is basically a least squares linear fit of the natural logarithm of the intensity versus airmass. If I_o can be determined by other means or if it remains stable from day to day (or night to night), then δ can be computed directly from the Bouguer-Beer-Lambert Law.

Information about the size distribution of atmospheric aerosols is contained in the wavelength dependence of extinction. Frequently the Ångström power law is used as a means of expressing this wavelength dependence, with a wavelength exponent of $-\alpha$. For very small particles or molecules, α approaches 4 (Rayleigh scattering). If the particles are much larger than the wavelength, α is nearly 0. Typical values of α found in urban atmospheres range from 1 to 2, depending on the mix of new particle production and aerosol growth processes as they age in the atmosphere. The most dramatic observable effect of aerosol light scattering is the shift in the color of the daytime sky from blue (predominantly Rayleigh scattering) to whitish gray.

While the measurement of solar or stellar intensities is straightforward in principle, actual instruments for doing so have become relatively complex, with computers controlling the measurement process as well as processing and recording the data. Solar radiometry and stellar photometry have been in use since the early 1960s. There are two types of solar radiometers: one actively tracks the sun and measures direct normal irradiance; another passively measures direct solar and diffuse irradiance on a horizontal plane. For the latter type, a shadowband is often used to separate the direct and diffuse components. Both types have been designed, built, and used at Pacific Northwest Laboratory (PNL): the mobile automatic spectral photometer (MASP) (Kleckner et al. 1981) and the rotating shadowband radiometer (RSR) (LeBaron et al. 1989). The heart of most solar radiometers is a silicon cell detector, often used in combination with interference filters for wavelength selection. For the stellar photometer, the silicon cell detector is replaced by a photomultiplier detector and the entrance to the photometer is placed at the focal plane of a telescope.

Historically, the application of solar and stellar radiometry for determining atmospheric extinction have had rather divergent objectives. Most solar radiometric observations are intended primarily for determining aerosol optical depth. On the other hand, most astronomers are intent on doing astronomy and do not have the time or interest to spend much time on extinction measurements and evaluating their uncertainties. Fortunately, there are some astronomers who have taken the time to make careful extinction measurements as a necessary part of some long-term photometric program. An example of such an effort is the Lowell Observatory program to measure comparison stars for the outer planets and some of their satellites (Lockwood and Thompson 1986).

Survey of Extinction Measurements

In this section, the observations of atmospheric light extinction since about 1960 to the present will be summarized. For the present, this survey is restricted to a rather limited set of articles that have reported on three relatively long-term measurement programs--namely, the Lowell Observatory (LO) outer planet photometry and solar variability program (Lockwood and Thompson 1986), the Pacific Northwest Laboratory (PNL) solar radiometry and atmospheric

turbidity study (Pearson et al. 1988; Michalsky et al. 1990), and the stratospheric aerosol observation work at the Fraunhofer Institute in Garmisch-Partenkirchen, Germany (Jäger 1991; Jäger 1992). The survey will summarize the major findings of the ASTRA work (Laulainen et al. 1977; Laulainen 1977; Taylor et al. 1977) as a way of introducing the intercomparison of the different data sets. As mentioned earlier, results from the ASTRA study revealed several major atmospheric light extinction features: seasonal variations, volcanic perturbations and time trends. Each of these features will be discussed in the next sections. Unless otherwise noted, the results pertain to observations made at a wavelength of 550 nm.

The LO photometric program to measure comparison stars for the outer planets and some of their satellites began in late 1972. Light extinction observations were a necessary and routine part of this long-term program. Results of 485 nights of photometric observations spanning a 13-year period from 1972-1985 were used by Lockwood and Thompson (1986) to examine the ordinary and volcanically induced variations in atmospheric extinction. The observations are particularly interesting and useful since the same photometer, interference filters, and list of standard stars fainter than a visual magnitude of 5.2 were used throughout the measurement program, which gives confidence in the intercomparability of the data over such a long time series. Furthermore, as described by Lockwood and Thompson (1986), "Flagstaff [in northern Arizona] is a good high altitude (elevation 2.2 km) astronomical site, free from anthropogenic influences upon the extinction." The results from this site should reflect the variations seen at other continental locations in the southwestern United States, including those from KPNO in southern Arizona.

The PNL solar radiometry program essentially began in 1974, when a series of observations of atmospheric turbidity were begun using hand-held, multi-filter sunradiometers. Observations were taken at the Hanford Meteorological Station (HMS, elevation 0.1 km) and the Rattlesnake Mountain Observatory (RMO, elevation 1.1 km) near Richland in southeastern Washington State. Development of a computer-controlled radiometer, the mobile automated spectral photometer (MASP) mentioned earlier, was begun about the same time. The MASP was put into service in 1978 at RMO and in about 1985 at HMS. The MASP can be programmed to measure

direct solar irradiance or to obtain a map of diffuse sky radiance in 12 spectral wavelengths (Kleckner et al. 1981), although only 5 wavelengths have been used for investigating atmospheric light extinction. In 1980, once the MASP was fully operational, the hand-held sunradiometer observations were discontinued.

Work also began in 1980 to automate a rotating shadowband radiometer (RSR), which used a fast-response silicon cell pyranometer for obtaining direct, diffuse and total solar irradiance on a horizontal surface (Michalsky et al. 1986). The RSR was later modified with a broadband filter centered at 555-nm wavelength for measuring illuminance (LeBaron et al. 1989). On clear days the direct component can be used to extract optical depth. More recently the RSR was redesigned for up to 7 independent spectral measurements using the same diffuser assembly for the incident radiation (Harrison 1991). The multi-filter/detector RSR (MFRSR) can be operated in a mode to obtain optical depths that are equivalent to the MASP units. A comparison of aerosol optical depths obtained with each instrument during 1991 is shown in Figure 1. Although the wavelength bands for the two instruments are not the same, the interpolated δ_{ep}-values agree to within 0.01.

A 14-year (since 1978) time series of aerosol optical depths using the MASP is available at PNL. Results from this long-term observational period have appeared on two occasions: one describing the 8-year period, 1978-1986 (Pearson et al. 1988), and one describing the 10-year period, 1978-1988 (Michalsky et al. 1990). There is good overlap between the LO and PNL data sets and both include the period of the El Chichon eruption.

At Garmisch-Partenkirchen (GP), the stratospheric aerosol layer has been studied by backscatter lidar since 1976 (Jäger 1991). The lidar system consists of a pulsed ruby laser emitting at 694.3 nm and a 52-cm-diameter Cassegrain telescope as receiver. Height resolution of the system is about 600 m with a lower altitude range of about 7 km. The average frequency of observation is once per week. The GP lidar observation station and the PNL solar radiometric site are at approximately the same latitude (47.5 deg N and 46.4 deg N, respectively). The stratospheric backscatter profiles are important to the interpretation of

the solar and stellar extinction measures as a means for getting an independent measure of stratospheric optical depth and mass loading, especially during the volcanically perturbed periods. The lidar measures the integrated backscatter ratio, which can be converted to optical depth using extinction to backscatter ratios determined from a stratospheric aerosol model; a value of 50 is typical for wavelengths near 694 nm. Michalsky et al. (1990) used both the GP lidar results and those from the NASA-Langley lidar (McCormick et al. 1984) and the NOAA-Mauna Loa lidar (DeLuisi et al. 1985) in the interpretation of their work, while Lockwood and Thompson (1986) used the results of the NASA-Langley lidar and the NOAA-Mauna Loa lidar.

Seasonal Variability

At most locations examined in the ASTRA study, there were definite seasonal periodicities in the data, while at some locations there was either very little variation about the yearly mean or there were large excursions from the yearly mean for which no seasonal effect was apparent. For those locations with definite seasonal variations, the amplitudes of the excursions were typically in the range of 0.01-0.03 optical depth units with a mean around 0.02 and the phase of the maximum occurring in the local spring and summer months. Figure 2 shows data from KPNO, McDonald Observatory, and Lick Observatory during the period 1959-1970. Daily fluctuations at many sites could show excursions of up to 0.1 to 0.2 optical depth units or even larger (Laulainen et al. 1977).

Most of this variability was attributed to aerosol mass loading changes in the lower troposphere as a result of biogenic activity and/or seasonal atmospheric circulation patterns bringing in airmasses that were impacted by human activity, wind-blown dust, or relatively high moisture content. Generally the seasonal variations were larger in the Northern Hemisphere (NH) than in the Southern Hemisphere (SH), consistent with the fact that anthropogenic emissions are much larger in the NH than in the SH (Charlson et al. 1992). Recent evidence suggests that the seasonal patterns of aerosol loading in the lower troposphere, i.e., the spring-summer maximum, are driven by the photochemical reactivity of the atmosphere and distribution patterns of key aerosol precursor gas emissions (Chang et al. 1990).

The LO extinction time-series spanned periods of significant volcanic activity and a relatively quiescent period. The near absence of volcanically produced stratospheric aerosol during the years 1976-1980 allowed Lockwood and Thompson (1986) to establish a seasonally variable background tropospheric aerosol light extinction pattern that could then be used to compare with the volcanically active period after 1980. The spring-summer maximum found in this pattern, shown in Figure 3, is consistent with the seasonal pattern for KPNO during the 1960s (Laulainen et al. 1977). The aerosol extinction during the high extinction months (March-July) was about 0.05, while in the low months (December-February) it was usually <0.02, implying that the amplitude of the seasonal variation from the mean is about 0.015 or roughly half of the amplitude reported for KPNO. Substantial dispersion in the extinction coefficients as a result of variations in tropospheric conditions were also observed, with the greatest dispersion (±0.025) occurring in the high extinction months.

The situation for the Rattlesnake Mountain Observatory (RMO) extinction time series is very similar, in many respects to the LO time series. Both span a similar period and used a similar time period for establishing a seasonal background (1978-1981 at RMO, cf. Michalsky et al. 1990). Perhaps more importantly is that both show the same phase and a similar magnitude of the spring-summer extinction maximum, even though the two sites are widely separated in latitude and there is a 1 km difference in site elevation. The seasonally variable background tropospheric aerosol light extinction pattern at RMO is shown in Figure 4. At 535 nm, the mean annual aerosol optical depth is 0.05 and the magnitude of the seasonal variation from the mean is about 0.025. The dispersion in the PNL data, however, is perhaps twice that observed at LO, with the greatest dispersion occurring in the high extinction months.

No seasonal variations are apparent in the GP stratospheric data.

Volcanic Perturbations

The ASTRA work did not explicitly look at volcanic perturbations to atmospheric extinction, although its timeframe included the Mt. Agung eruption in March 1963. In most cases, the seasonal and trend analyses excluded the time period

of maximum perturbation (1963-1964). Much of the Agung perturbation appeared to be confined to the SH. For example, at the one site in South Africa (Boyden Station), where calculations were done with and without the Agung perturbation, the effect was to increase the average annual extinction by about 0.04 over the 8-year observation period (1957-1965).

The perturbations in the extinction data from LO and PNL resulting from volcanic eruptions, especially the larger ones such as El Chichon, are generally recognizable even in the raw data. However, with appropriate data processing, such as removing the background seasonal tropospheric aerosol component and applying data-smoothing and curve-fitting techniques, the remaining time-series can clearly show even the smaller perturbations, as shown in Figure 5. The El Chichon perturbation was significant, as shown in Figures 6 and 7, from the standpoint of duration of the stratospheric aerosol cloud (>2 years) and the magnitude of the optical depth change (0.10-0.12) (Lockwood and Thompson 1986; Michalsky et al. 1990). Early indications are that the Pinatubo perturbation, also shown in Figure 7, may produce twice the optical depth change (~0.2) as El Chichon (Larson et al. 1992).

The effects of volcanic perturbations to the stratosphere are easily discerned in the lidar backscatter ratios. Indeed, as mentioned earlier, lidar backscatter data are often used to interpret changes in the total atmospheric extinction. Again the interesting features of the El Chichon event, as shown in Figure 8, are its duration (>2 years) and the magnitude of the change (~100-fold increase in the backscatter ratio) (Jäger 1991). While it is too early to estimate the effects of Mt. Pinatubo, the lidar observations indicate some significant differences between it and El Chichon, as illustrated in Figure 9. These differences may be the result of either a faster northward transport and/or a greater mass of the Pinatubo aerosol cloud as it reached the GP site (Jäger 1992). These differences are also apparent in the RMO data shown in Figure 7, when the rate of increase in aerosol optical depth between the two events are compared.

Aerosol Loading Trends

Careful trend analysis was performed over the period 1960-1972 for four observatory sites in the ASTRA work: CTIO, KPNO, Lick Observatory, and McDonald Observatory. No conclusion was drawn for any trend at CTIO because of insufficient data after the Agung years were excluded. Of the remaining three observatories, when averaged together, a weak trend of 0.01 ± 0.01 was found. The large uncertainty in this result includes the possibility of no trend also.

No attempt has been made, as yet, to analyze either the LO or the PNL data for trends. Part of the difficulty stems from the manner in which the data were processed to extract the seasonal extinction variation. Since several years of data were aggregated to develop the seasonal statistics and curve-fit, it is somewhat dubious to return to that same time series to attempt to find a trend. The other time periods of the data were essentially masked by the relatively large volcanic perturbations.

The situation is somewhat different for the GP lidar data (see Figure 8), where an increase in the stratospheric background particle backscatter of about 8% per year since 1979 (constructed from data without volcanic perturbation) seems to have occurred (Jäger 1991). Jäger (1991) suggests that this steady increase may be the result of direct anthropogenic emissions into the stratosphere, such as from aircraft. At the moment, such an effect would be difficult to detect, the Pinatubo eruption notwithstanding, using the solar or stellar photometric observations, since the change in stratospheric aerosol optical depth between 1979 and 1990 as a result of the inferred GP background aerosol optical depth change would amount to only about 0.003, which is much smaller than the value of 0.01 considered to be detectable by the present PNL statistical analysis method.

Wavelength Dependence of Extinction

The earlier ASTRA papers dealt mainly with broadband optical extinction at 550 nm. Photometric observations were available at a few other wavelengths, depending on which photometric system was used. In the paper by Taylor et al. (1977), a great deal of effort was spent deriving correction factors to convert the extinction coefficients obtained in the UBV broadband system to monochromatic values. For the broadband V filter (nominally at 550 nm) the

corrections were minor, but in the broadband B filter (nominally at 442 nm) the corrections were quite sensitive to stellar type. Extinction results in the U filter were not considered. In the analysis, trends in the B extinction were found to be somewhat smaller than in the V extinction, but the large uncertainties in both the B and V trends precludes any meaningful conclusions about trends in the wavelength dependence of extinction and, therefore, particle size.

Lockwood and Thompson (1986) used a different color system, the "ubvy" narrow-band system, for their observations. They reported results for light extinction in the b and v bands at 470 nm and 550 nm, respectively, with the extinction color difference given as the difference between b- and v-band extinction κ_{b-v}. Mean extinction color differences at LO for the seasonal background aerosol (see Figure 3) were about 0.055, with the differences increasing by about 0.01 during the spring-summer v-band extinction maximum (implying freshly produced smaller particles) and decreasing by about 0.01 during the winter months (implying somewhat larger, well-aged particles). For the volcanic events observed at LO, the extinction color difference, as shown in Figure 6, initially increased by as much as 0.02 or more in the El Chichon case and quickly decreased to values <0. These changes again reflect the evolution of the stratospheric aerosol cloud from freshly-produced smaller particles to larger, aged-aerosol. The El Chichon event also showed interesting annual cycling of the extinction color difference, with large positive values (0.02) in the fall and negative values (in the range -0.01 to 0) in late winter.

Aerosol optical depths at RMO (Michalsky et al. 1990) were derived from observations at 5 wavelengths (namely at 428, 486, 535, 785, and 1010 nm, respectively). The wavelength dependence of extinction of the seasonal background aerosol and the volcanic perturbations was determined from the slope of a least squares fit to the Ångström power law relationship using these data. Qualitatively, the wavelength dependence of the seasonal background tropospheric aerosol extinction at RMO, as shown in Figure 4, is consistent with that observed at LO--namely, smaller values of α in the winter months and larger values in the spring and summer months, even though the two sites are widely separated geographically and are at different elevations.

As seen in Figure 7, the wavelength exponent α was about 1.1 prior to the Mt. St. Helens eruption and decreased to just under 1 before the Alaid eruption. Thereafter, a general trend of increasing values of α (decreasing particle size) until 1982 occurred, reaching a value of about 1.4. The El Chichon eruption had a dramatic effect on mean particle size, with α dropping abruptly to about 0.4 at peak loading, implying a substantial increase in particle size. As the El Chichon aerosol cloud decayed, α slowly returned to its pre-eruption value. Superimposed on the slow increase was an apparent shift to larger particles, with α decreasing by about 0.1 each winter, beginning in 1985. Because the calculations of α were based on the total atmospheric column, the explanation of this effect is still uncertain, since the possibility exists that these variations may be the result of increases in tropospheric aerosol size in the winter months. In any case, the LO and PNL observations of the wavelength dependence of extinction for the volcanic events appear to be consistent.

The limited data, which are available at the present time, show that the Pinatubo eruption is producing qualitatively similar changes in the wavelength dependence of extinction. For the 2-3 years prior to the Pinatubo eruption in mid-1991, the mean background aerosol extinction in January and February had α-values around 0.7. In January and February 1992, the mean value of α was 0.4, similar to the lowest α-values observed during the El Chichon event.

Summary and Recommendations

Observations of atmospheric extinction provide a valuable source of information for evaluating potential climate forcing and visibility impairment resulting from atmospheric aerosols. Such observations are generally carried out during daylight hours using solar radiometry or by means of satellite and ground-based lidar remote-sensing techniques. In principle, nighttime extinction data are also available from various astronomical observations but, with the exception of a few individual efforts, few of them have found their way into more accessible data bases.

A major purpose of this paper was to illustrate the utility of astronomically-derived atmospheric light extinction data by comparing the results from two

studies of atmospheric transparency using stellar photometry techniques (the ASTRA work published in the mid-1970s and the long-term LO observing program) with a long-term study of multi-spectral solar irradiance and aerosol optical depths at PNL using solar radiometric methods. Several aspects of the time series data used in each of these studies were considered, including the seasonal dependence of light extinction and its wavelength dependence, perturbations to extinction and its wavelength dependence in the stratospheric aerosol layer by volcanic eruptions, and potential time trends in aerosol light extinction. It was shown that the data sets are quite compatible for examining these different features.

Another purpose of this paper was to describe, in a somewhat qualitative manner, how the optical depth and its wavelength dependence are related to parameters needed for estimating the magnitude of climate forcing due to anthropogenic aerosols, impacts on visibility, and, for the astronomer, the impact of aerosols on astronomical observing programs. A major question with respect to the climate change issue is the magnitude and distribution in time and space of aerosol forcing. This question can only be resolved realistically by thorough characterization of the distribution of aerosol optical depth over the planet by means of satellite observations. The satellite observations, however, need to be tied to ground-truth measurements, such as can be provided by a combination of solar and stellar photometric determinations of aerosol light extinction distributed worldwide and at different elevations (needed for independently assessing the contributions from the stratosphere).

Indeed, if the assertions of Charlson et al. (1992), with respect to the large increase in sulfur emissions that have occurred in the NH during the past 30 years and the (presumed) resulting increase in tropospheric sulfate aerosol burden, are correct, then a reexamination of the various time series of light extinction data is urgently needed to see if any trends in total atmospheric column burden can be detected over the 30-year period, 1960-1990. The lidar studies at GP, for example, suggest that the mean aerosol optical depth at 694 nm in the stratosphere may have increased by about 0.003 over the past 15 years, perhaps as a result of increasing air traffic over Europe. Trends of this magnitude may be difficult to detect when realizing that the amplitudes of the

seasonal variations lie in the range 0.02-0.04 with dispersions (day-to-day variability) in the range 0.02-0.05, depending on geographic location and altitude, or that volcanic perturbations may increase the optical depth by as much as 0.2, depending on the magnitude of the eruption.

In conclusion, there is a clear need to analyze as many data sets of atmospheric light extinction as possible to provide the IGBP/Global Change research community with a clearer picture of aerosol loading and optical properties for assessing potential climate change effects. Atmospheric extinction data archived by the astronomical community can play a valuable role in this activity, but more information is needed on what data are available and how these data may be obtained, compiled and analyzed without major disruption of the astronomer's own research programs. As suggested by Lockwood and Thompson (1986), an added benefit to the astronomer of such a compilation and analysis would be a means of deriving mean atmospheric extinctions coefficients that could be used in his observing programs. For the astronomer, observing at a good background site, it is interesting to note that light extinction excursions are largely controlled by volcanic eruptions and that other changes, beyond the seasonal variation, are not apparent above the noise resulting from day-to-day variability in aerosol loading.

Acknowledgments. I would like to express my appreciation to Dr. D. McNally for the invitation to present this paper at the IAU/ICSU/UNESCO exhibition and to the IAU for travel expenses to attend the meeting. My thanks also go to Dr. D. Crawford for providing me with contacts in the astronomical community, who have potential access to atmospheric extinction data. I would like to particularly thank Drs. J. Michalsky, W. Lockwood, and H. Jäger for useful discussions and kindly allowing me to use results from their publications in this presentation. This work was supported by the U.S. Department of Energy under Contract DE-AC06-76RLO 1830. Pacific Northwest Laboratory is operated for the U. S. Department of Energy by Battelle Memorial Institute.

References

Cleveland, W. S. 1979. "Robust locally-weighted regression and smoothing scatterplots." J. American Statistics Association 74: 829-836.

Chang, J. S., P. B. Middleton, W. R. Stockwell, C. J. Walcek, J. E. Pleim, H. Lansford, S. Madronich, D. Byun, J. N. McHenry, and H. Hass. 1990. The Regional Acid Deposition Model and Engineering Model. Acidic Deposition: State of Science and Technology Report No. 4, National Acid Precipitation Assessment Program, Washington D. C.

Charlson, R. J., S. E. Schwartz, J. M. Hales, R. D. Cess, J. A. Coakley, Jr., J. E. Hansen, and D. J. Hofmann. 1992. "Climate forcing by anthropogenic aerosols." Science 255: 423-430.

DeLuisi, J. J., E. G. Dutton, K. L. Coulson, and F. Fernald. 1985. "Lidar observations of stratospheric aerosol over Mauna Loa Observatory: 1982-1983." Data Report ERL ARL-5, NOAA, Silver Spring, Maryland.

Harrison, L. C. 1991. "Multi-spectral automated rotating shadowband radiometry in the Atmospheric Radiation Measurements (ARM) Program." In Proceedings of the Biennial Congress of the International Solar Energy Society Meeting, eds. M. E. Arden, S. M. A. Burley, and M. Coleman, pp. 893-898. Pergamon Press, New York.

Jäger, H. 1991. "Stratospheric aerosols: Observations, trends and effects." J. Aerosol Science 22 (Suppl. 1): S517-S520.

Jäger, H. 1992. "The Pinatubo eruption cloud observed by lidar at Garmisch-Partenkirchen." Geophysical Research Letters 19: 191-194.

Kleckner, E. W., J. J. Michalsky, L. L. Smith, J. R. Schmelzer, R. H. Severtsen, and J. L. Berndt. 1981. "A multi-purpose computer-controlled scanning photometer." PNL-4081, Pacific Northwest Laboratory, Richland, Washington.

Larson, N. R., E. W. Kleckner, J. J. Michalsky, L. C. Harrison, and D. Nelson. 1992. "Mount Pinatubo stratospheric aerosol perturbation measured by northern mid-latitude solar photometers." Presented at the Spring AGU Meeting, Montreal, 11-15 May.

Laulainen, N. S. 1977. "Analyses of atmospheric extinction data obtained by astronomers--III. Compilation of optical depths for 31 observatory sites." Atmospheric Environment 11: 29-33.

Laulainen, N. S., B. J. Taylor, and P. W. Hodge. 1977. "Analyses of atmospheric extinction data obtained by astronomers--II. Seasonal variations in astronomical extinction." Atmospheric Environment 11: 21-27.

LeBaron, B. A., J. J. Michalsky, and L. Harrison. 1989. "Rotating shadowband photometer measurement of atmospheric turbidity: A tool for estimating visibility." Atmospheric Environment 23: 255-263.

Lockwood, G. W., and D. T. Thompson. 1986. "Atmospheric extinction: The ordinary and volcanically induced variations, 1972-1985." Astronomical Journal 92: 976-985.

McCormick, M. P., T. J. Swissler, W. H. Fuller, W. H. Hunt, and M. T. Osborn. 1984. "Airborne and ground-based lidar measurements of the El Chichon stratospheric aerosol from 90 deg N to 56 deg S." Geofisica Internacional 23: 187-221.

Michalsky, J. J., J. L. Berndt, and G. J. Schuster. 1986. "A microprocessor-based rotating shadowband radiometer." Solar Energy 36: 465-470.

Michalsky, J. J., E. W. Pearson, and B. A. LeBaron. 1990. "An assessment of the impact of volcanic eruptions on the Northern Hemisphere's aerosol burden during the last decade." J. Geophysical Research 95D: 5677-5688.

Pearson, E. W., B. A. LeBaron, and J. J. Michalsky. 1988. "Decay of the El Chichon perturbation to the stratospheric aerosol layer: Multispectral ground-based radiometric observations." Geophysical Research Letters **15**: 24-27.

Taylor, B. J., P. B. Lucke, and N. S. Laulainen. 1977. "Analyses of atmospheric extinction data obtained by astronomers--I. A time-trend analysis of data with internal accidental errors obtained at four observatories." Atmospheric Environment **11**: 1-19.

List of Figures

Figure 9. Comparison of the lidar-derived column aerosol backscatter time series, in days after eruption, for the El Chichon and Pinatubo events. The curves show pronounced differences in the evolution of the aerosol cloud for the two events as observed at the GP site.

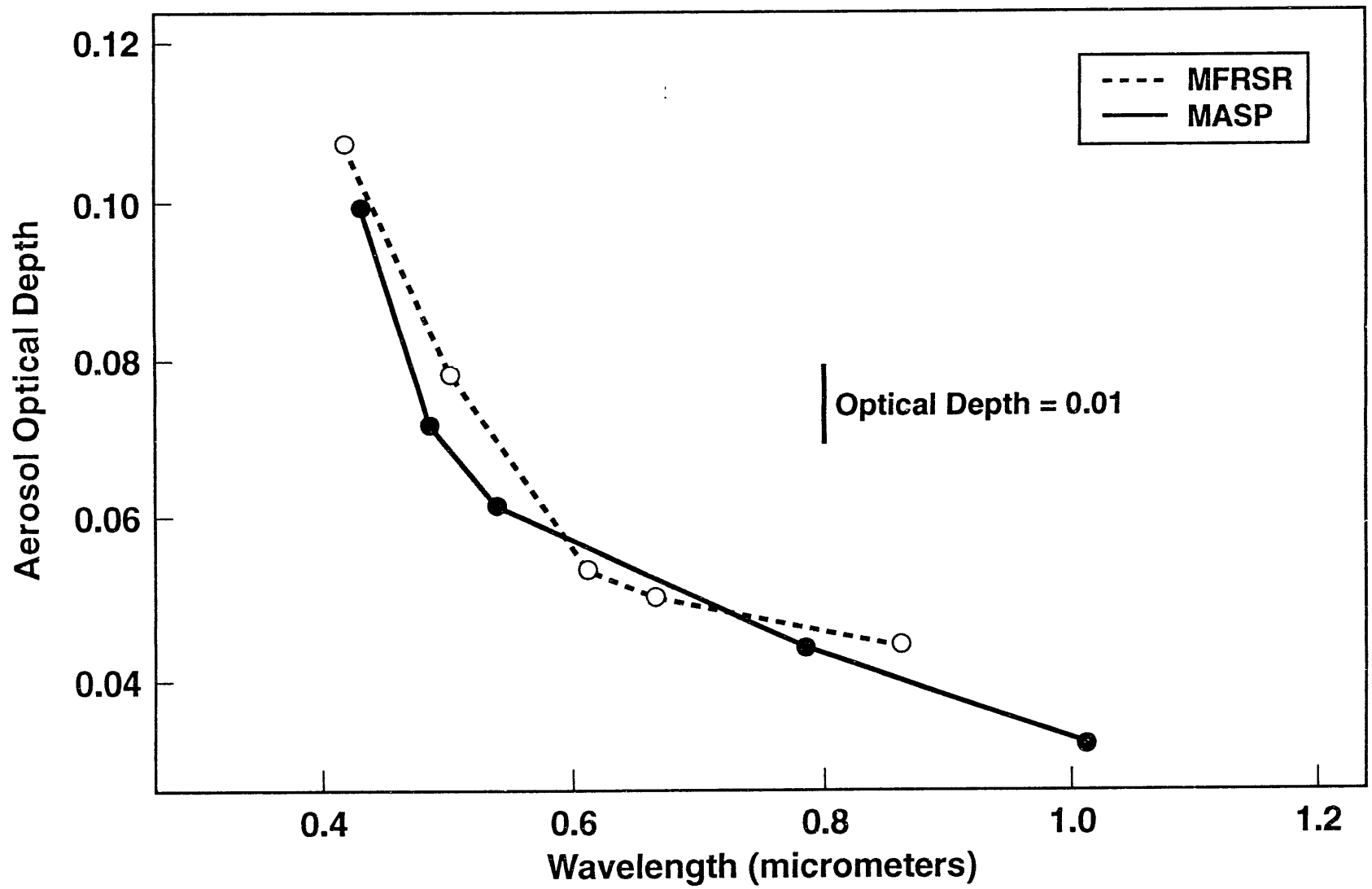
0.12
0.10
0.08
0.06
0.04
Aerosol Optical Depth
MFRSR
MASP
Optical Depth = 0.01
0.4
0.6
0.8
1.0
1.2
Wavelength (micrometers)
S9208053.7

Fig 1

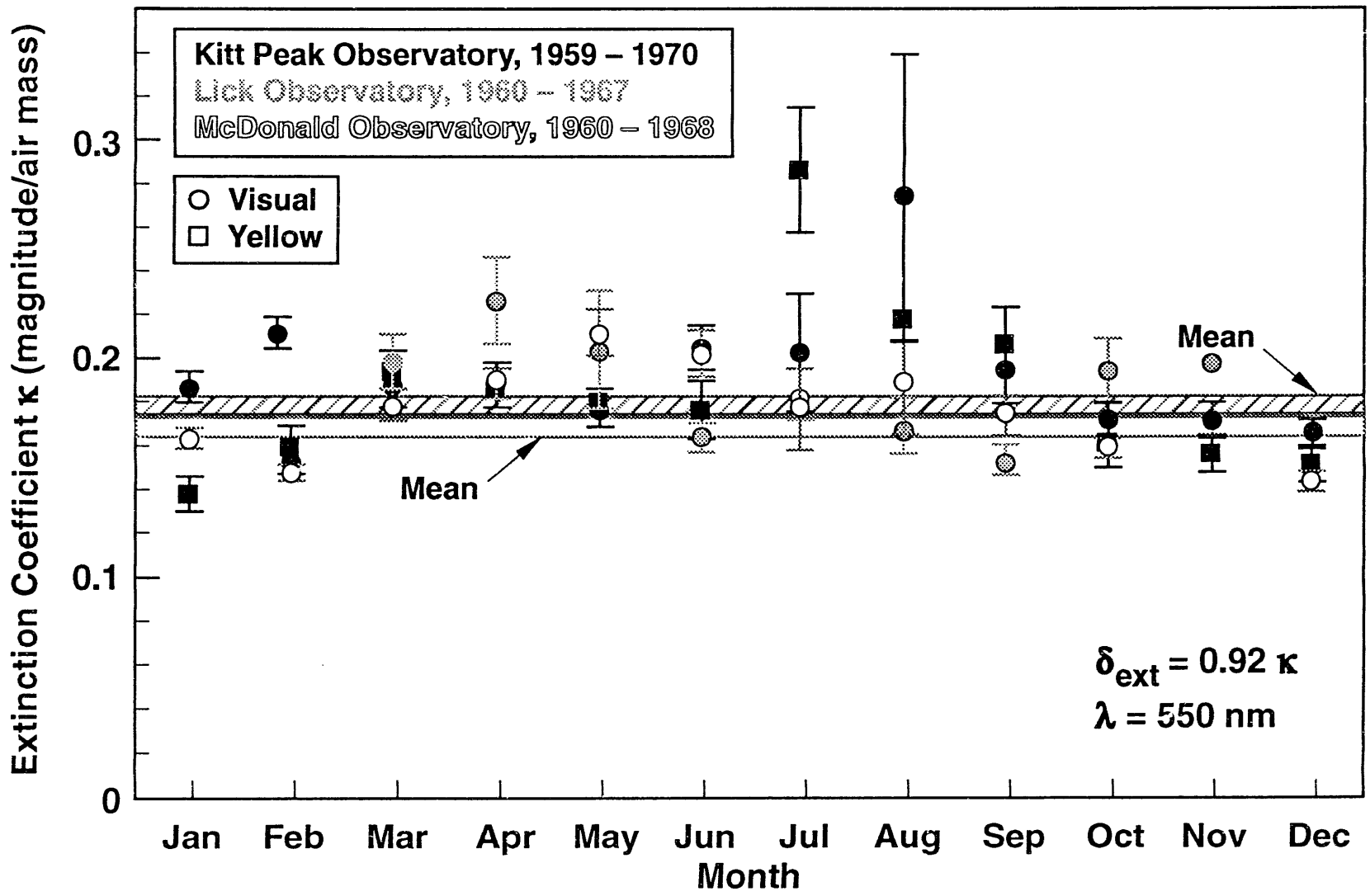
Kitt Peak Observatory, 1959 – 1970
Lick Observatory, 1960 – 1967
McDonald Observatory, 1960 – 1968
Visual
Yellow
Mean
Mean
$\delta_{ext} = 0.92\ \kappa$
$\lambda = 550$ nm
Extinction Coefficient κ (magnitude/air mass)
0
0.1
0.2
0.3
Jan
Feb
Mar
Apr
May
Jun
Jul
Aug
Sep
Oct
Nov
Dec
Month
S9208053.8

Fig 2

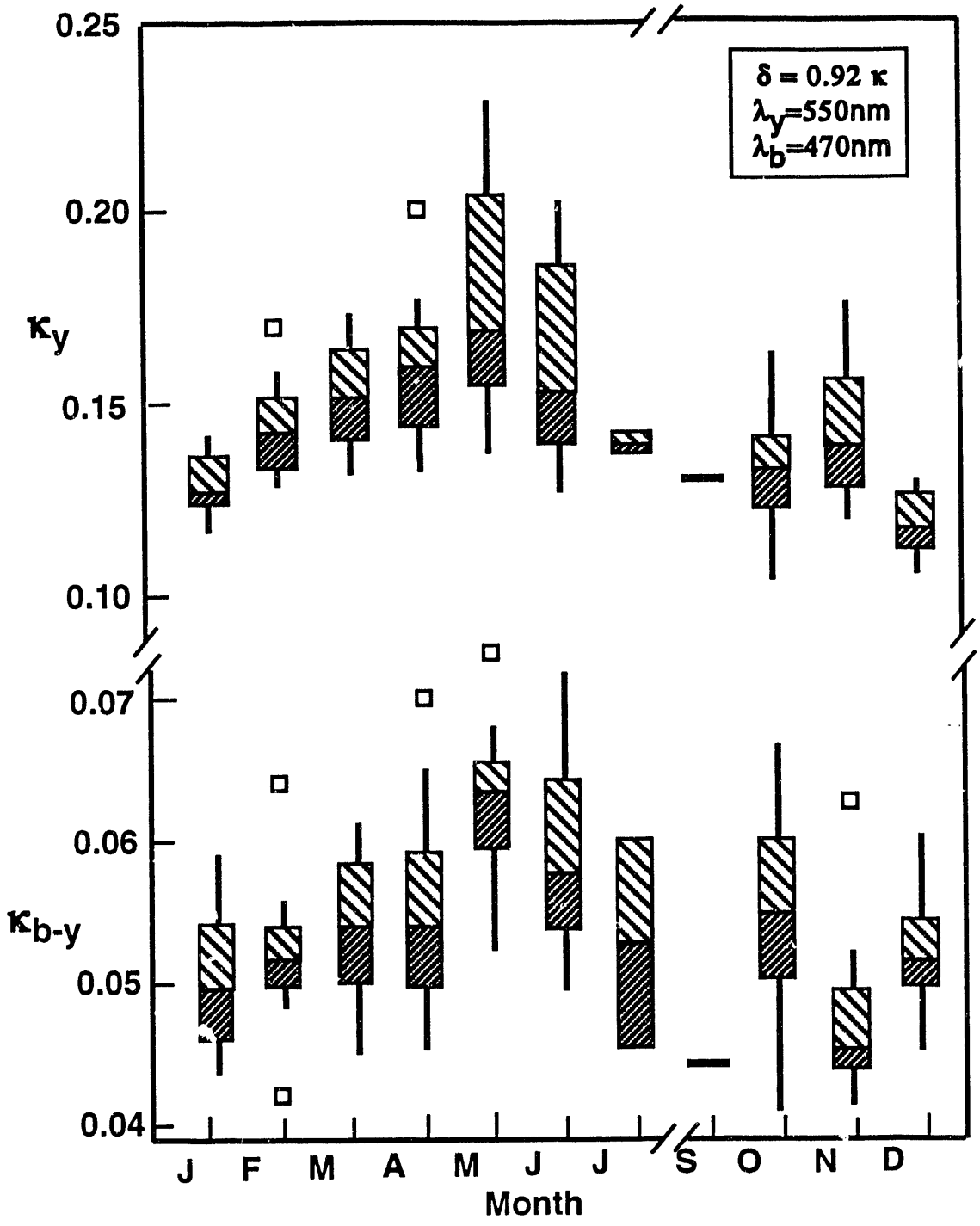

(Adapted from Lockwood and Thompson, 1986)

S9208053.9

Fig 3

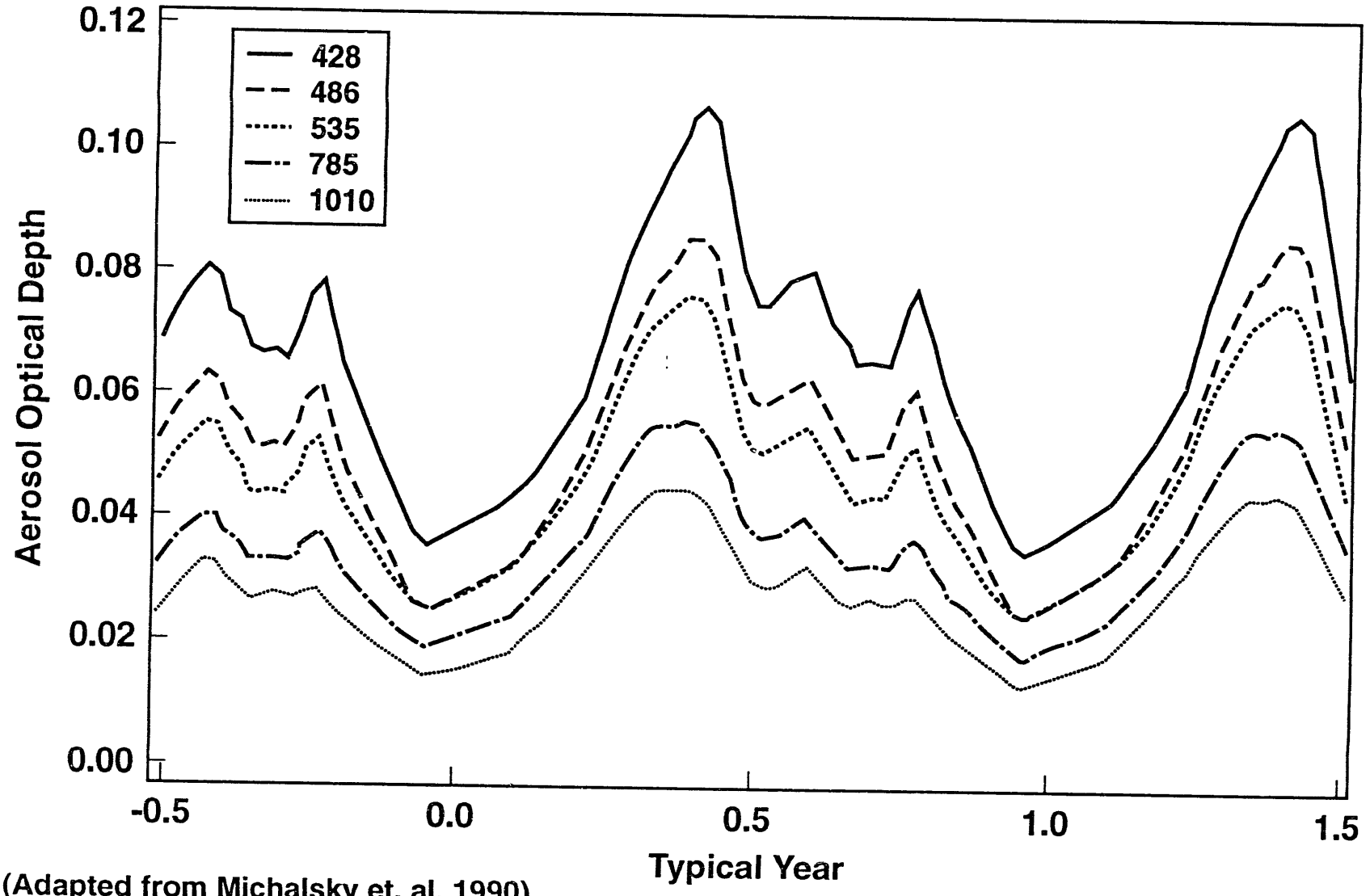

(Adapted from Michalsky et. al. 1990)

S9208053.5

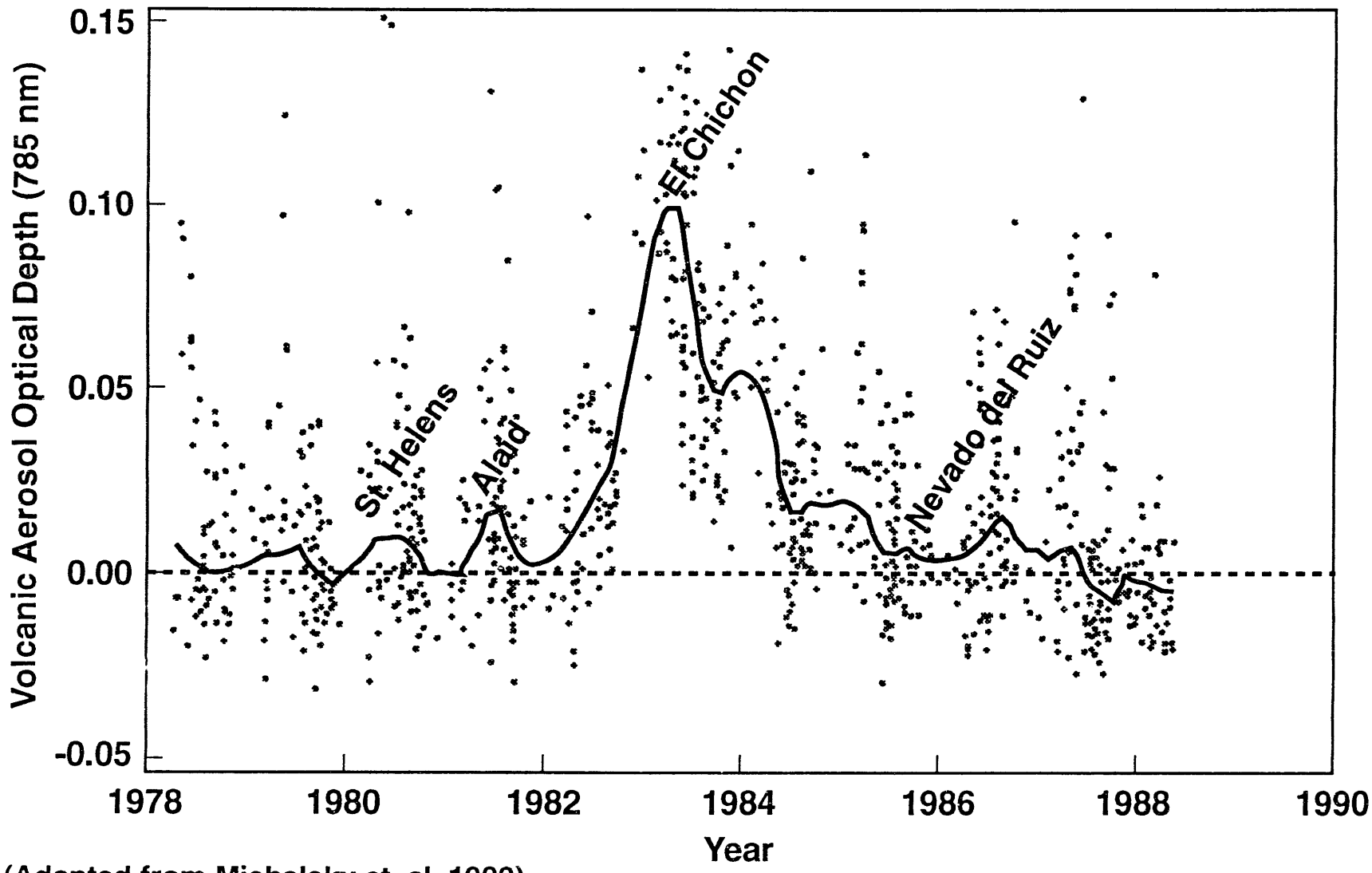

(Adapted from Michalsky et. al. 1990)

S9208053.4

Fig 5

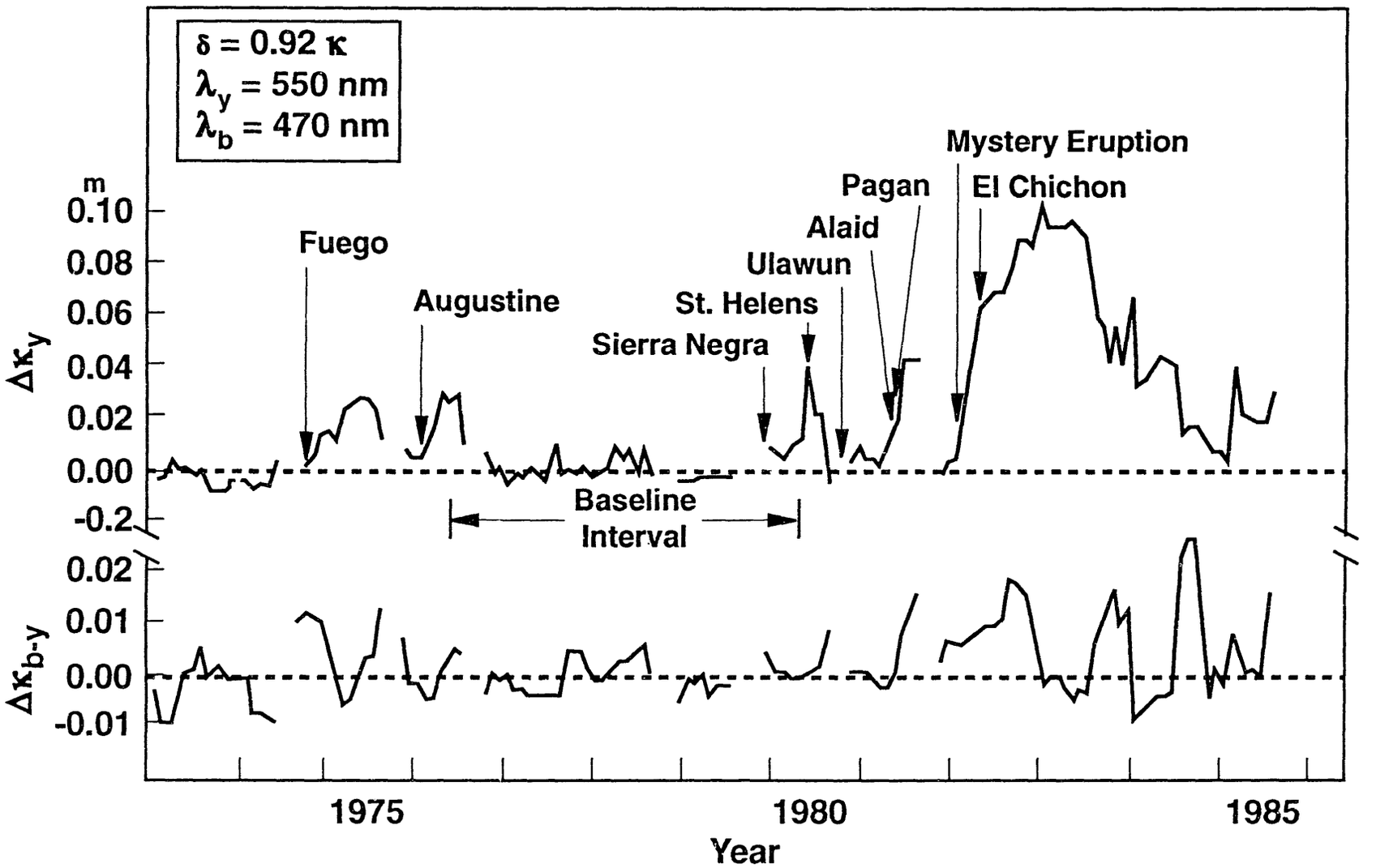

(Adapted from Lockwood and Thompson, 1986)

S9208053.1

Fig 6

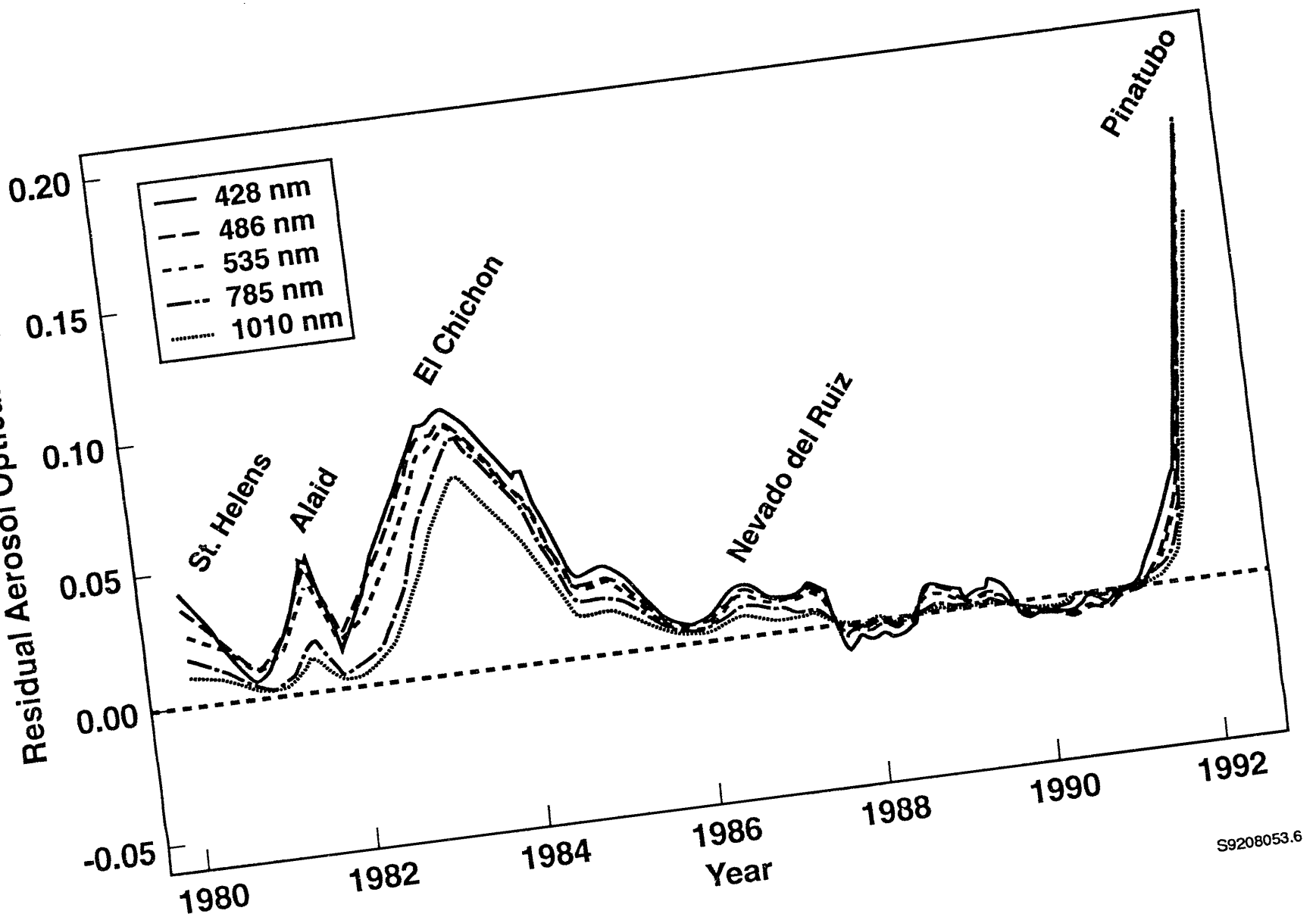
428 nm
486 nm
535 nm
785 nm
1010 nm
Residual Aerosol Optical Depth
0.20
0.15
0.10
0.05
0.00
-0.05
St. Helens
Alaid
El Chichon
Nevado del Ruiz
Pinatubo
1980
1982
1984
1986
1988
1990
1992
Year
S9208053.6

Fig

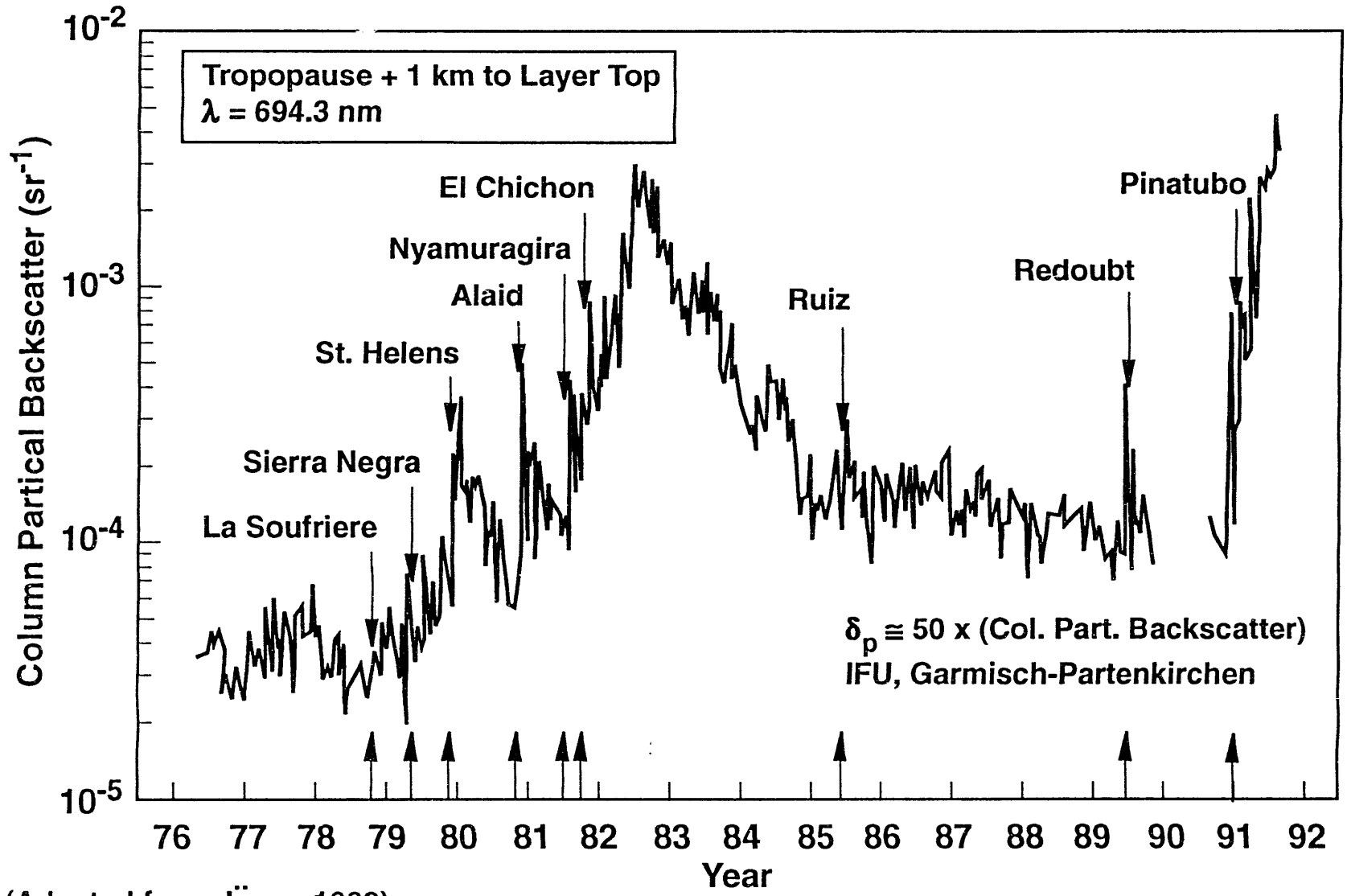

(Adapted from Jäger, 1992)

S9208053.3

Fig 8

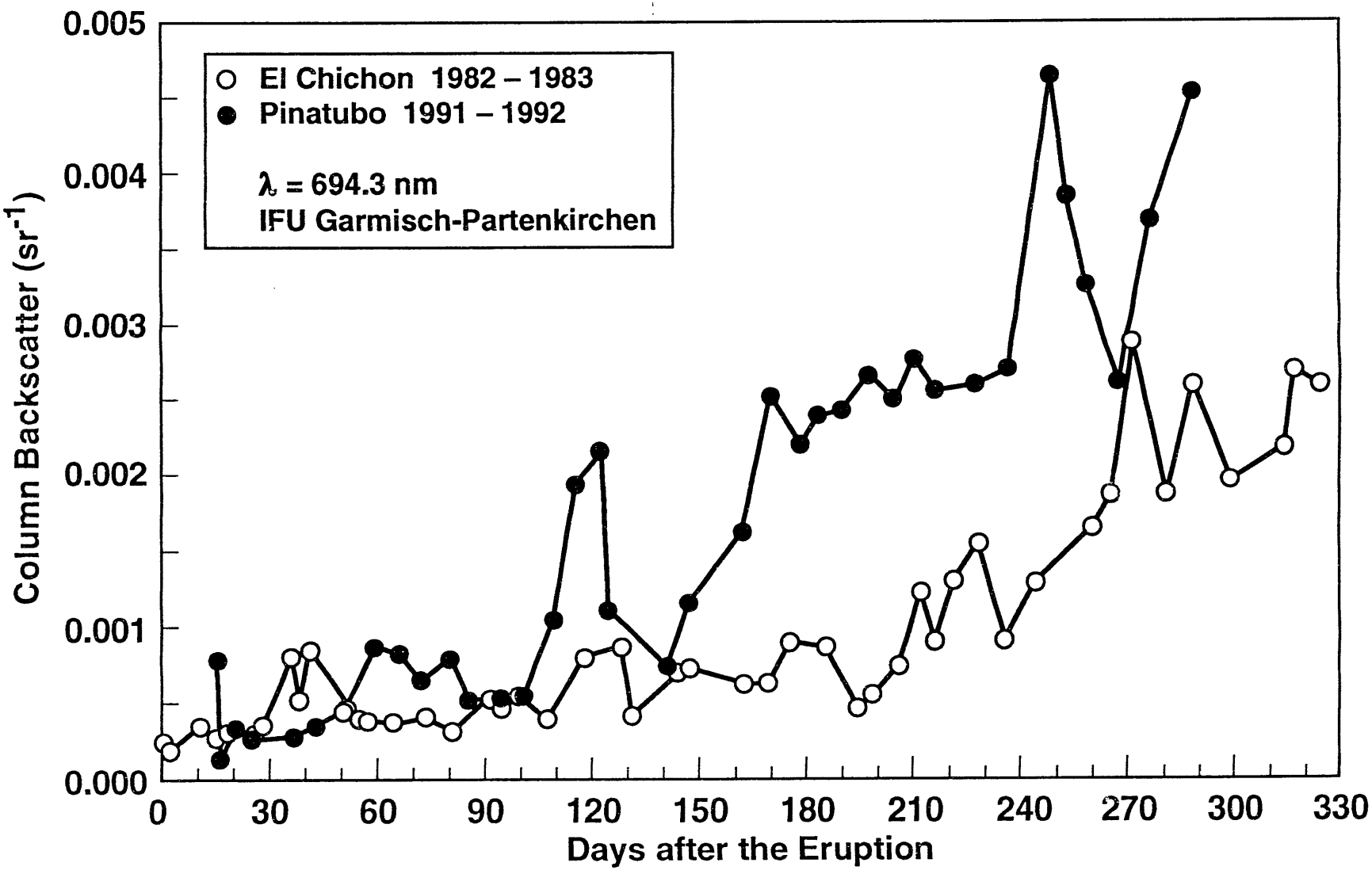

(Adapted from Jäger, 1992)

S9208053.2

Fig 9

END

DATE
FILMED
3/4/93